Measurement of transverse Λ and $\bar{\Lambda}$ hyperon polarization in pPb collisions at $\sqrt{s_{NN}} = 5.02$ TeV

R. Aaij *et al.*[*]
(LHCb Collaboration)

(Received 11 August 2025; accepted 10 November 2025; published 24 December 2025)

The transverse polarization of Λ and $\bar{\Lambda}$ hyperons is measured in pPb collisions collected by the LHCb experiment at a nucleon-nucleon center-of-mass energy of 5.02 TeV. The polarization is averaged over hyperon transverse momentum in the range $0.15 < p_T < 6.00$ GeV/c, and Feynman-x in the ranges $0.005 < x_F < 0.040$ (forward region) and $-0.10 < x_F < -0.01$ (backward region) defined relative to the proton beam direction. The transverse polarization is found to be compatible with zero for both Λ and $\bar{\Lambda}$ hyperons. The results are also measured as a function of p_T and x_F with no significant dependence on these variables observed. The results are compared with previous experimental measurements at different center-of-mass energies and collision environments.

DOI: 10.1103/rc6r-zt9q

I. INTRODUCTION

Spontaneous transverse polarization in the production of Λ baryons, with values up to 30%, was first measured nearly 50 years ago in unpolarized proton-proton (pp) and proton-nucleus collisions [1,2], which contradicted early leading-order perturbative QCD calculations [3], implying that the polarization must be due to nonperturbative aspects of QCD interactions. Since the first observation of transverse Λ polarization in hadron-hadron collisions, numerous experiments have explored this polarization using various beams and targets at different energies [4–12]. The observed polarization is negative, shows little dependence on the beam energy, and increases with Feynman-x, $x_F = 2p_z^*/\sqrt{s_{NN}}$, where p_z^* is the longitudinal momentum of the hyperon in the center-of-mass frame, and transverse momentum, p_T, up to a few GeV/c. Transverse polarization of the Λ baryon has also been observed with beams other than protons, such as γ, $K^{\pm}$, $\pi^{\pm}$, Σ^-, ν_μ, and neutrons on a target, as well as in semi-inclusive deep inelastic scattering [13–23]. For reviews of experiments and results, see for example Refs. [24–27]. The observation of Λ polarization has motivated theoretical investigations over several decades to understand transverse spin effects in hadron physics [3,27–33]. More recently, transverse polarization of both Λ and $\bar{\Lambda}$ baryons has been observed in e^+e^- collisions by the Belle and BESIII collaborations [34,35]. Belle observes that the polarization increases with the momentum fraction of the outgoing (anti)quark carried by the (anti)hyperon. Since there is no initial-state hadron in e^+e^- collisions, a hadronization effect must be present.

Spontaneous polarization of different hyperons has been measured in unpolarized hadronic collisions, as reviewed in Ref. [26]. A similar polarization trend as that for the Λ baryon has been observed for the Ξ^0 and Ξ^- states [6,36], and with opposite sign for the Σ^+, Σ^-, and Σ^0 baryons [37–39]. The polarization has also been studied when the detected hyperons do not have valence quarks in common with the proton beam in unpolarized hadronic collisions, and while zero polarization was observed for the $\bar{\Lambda}$ and Ω^- hyperons [2,40], nonzero polarization was found for the $\bar{\Xi}^+$ and $\bar{\Sigma}^-$ antibaryons [41,42].

In phenomenological frameworks describing transverse Λ polarization in unpolarized collisions, the polarization originates from the nonperturbative elements in the factorization expansion of the cross section. One well-established approach involves the polarizing transverse-momentum-dependent (TMD) fragmentation function (FF) [29–31,43,44], which describes the probability that an unpolarized quark fragments into a transversely polarized hadron. In unpolarized hadronic collisions, transverse polarization can arise from the convolution of TMD parton distribution functions and TMD FFs. The polarizing TMD FF has recently been extracted through fits to the measurement by the Belle experiment [34,45–47]. In hadron-hadron collisions, measurements of Λ polarization within jets offer a promising avenue to access the corresponding polarizing TMD jet FF [48–52].

[*]Full author list given at the end of the article.

An alternative, complementary formalism is provided in the collinear approach at higher orders in the factorization expansion, which allows for the description of spin asymmetries without the need for transverse momentum or jet reconstruction. In this framework, transverse polarization arises from quark-gluon-quark and three-gluon correlators [53,54], which encode spin-momentum correlations that can lead to a net transverse polarization of hyperons in unpolarized hadron-hadron collisions. This formalism has been used to compute contributions to the polarized hyperon cross section in unpolarized pp collisions, offering insight into the mechanisms responsible for the observed Λ polarization [54–58].

Hyperons decay via the weak interaction with non-conserved parity, permitting the measurement of their polarization by analyzing the angular distribution of their decay products. In the case of the $\Lambda \to p\pi^-$ decay, the transverse polarization is measured normal to the production plane, $\hat{n} = \hat{p}_{\rm beam} \times \hat{p}_\Lambda$, where $\hat{p}_{\rm beam}$ is aligned with the beam in the direction of the LHCb detector z-axis [59], and $\hat{p}_\Lambda$ is the direction of the Λ momentum in the laboratory frame. The observed angular distribution for the $\Lambda \to p\pi^-$ decay is given by

$$\frac{1}{N}\frac{\mathrm{d}N}{\mathrm{d}\cos\theta^*} = (1 + \alpha_\Lambda P_\Lambda \cos\theta^*)\varepsilon_{\rm tot}(\cos\theta^*), \qquad (1)$$

where N is the signal yield; θ^* is the angle between $\hat{n}$ and the decay proton momentum in the Λ rest frame; $\alpha_\Lambda = 0.746 \pm 0.009$ ($\alpha_{\bar{\Lambda}} = -0.757 \pm 0.004$) [60] is the parity-violating decay asymmetry; P_Λ is the polarization magnitude of the Λ; and $\varepsilon_{\rm tot}(\cos\theta^*)$ is the total efficiency, including reconstruction, selection, and acceptance effects that are determined from an unpolarized simulation a simulation without polarization effects through the detector. Polarization is determined through a binned linear fit of the efficiency-corrected $\cos\theta^*$ distribution. Similarly, for the $\bar{\Lambda}$ antibaryon, the angle between $\hat{n}$ and the decay antiproton momentum is determined.

In this paper, the transverse polarization of Λ and $\bar{\Lambda}$ baryons is measured as a function of $x_{\rm F}$ and $p_{\rm T}$ in pPb collisions at the center-of-mass energy in the nucleon-nucleon system $\sqrt{s_{\rm NN}} = 5.02$ TeV. The pPb measurement covers the backward rapidity range $-5.0 < y^* < -2.5$, in which the lead beam enters the LHCb detector at the interaction point, and the forward rapidity range $1.5 < y^* < 4.0$, where the proton beam enters the LHCb detector at the interaction point. Here, y^* is defined in the nucleon-nucleon center-of-mass system and is related to the rapidity in the laboratory frame by $y^* = y_{\rm lab} - 0.465$ in the forward configuration, and $y^* = -(y_{\rm lab} + 0.465)$ in the backward configuration. This measurement covers a poorly explored kinematic range and a much higher center-of-mass energy per nucleon than previous results, probing the Λ and $\bar{\Lambda}$ transverse polarization for $0.15 < p_{\rm T} < 6.00$ GeV/c, as well as $0.005 < x_{\rm F} < 0.040$ in the forward configuration and $-0.10 < x_{\rm F} < -0.01$ in the backward configuration. In symmetric collisions, such as pp, the polarization must be zero at $x_{\rm F} = 0$ and an antisymmetric function of $x_{\rm F}$, $P(-x_{\rm F}) = -P(x_{\rm F})$. In measurements using pPb collisions, the polarization is expected to be consistent with zero at $x_{\rm F} \approx 0$, as observed in previous experiments [11,12,61], and any nonzero polarization is likely to arise from nuclear effects.

II. DETECTOR, DATA, AND SIMULATION

The LHCb detector [62,63] is a single-arm forward spectrometer covering the pseudorapidity range $2 < \eta < 5$. The detector elements that are particularly relevant to this analysis are a silicon-strip vertex detector surrounding the pPb interaction region; a tracking system that provides a measurement of the momentum, p, of charged particles; and two ring-imaging Cherenkov (RICH) detectors that can discriminate between different species of charged hadrons. The polarity of the detector dipole magnet is reversed periodically during data taking, and the corresponding datasets are added together for this measurement. The corresponding integrated luminosity for the forward (backward) pPb data sample used for these results is 1.14 ± 0.02 nb^{-1} $(0.45 \pm 0.01$ nb$^{-1})$. Events are selected by a minimum-bias trigger that requires at least one reconstructed track in the vertex detector. A further requirement of at least one reconstructed primary vertex (PV) is imposed. Simulated events are used to model the effects of the detector acceptance and the selection requirements. In the simulation, pPb collisions are generated using EPOS-LHC event generator with a specific LHCb configuration [64], with 15×10^6 events generated for both the forward and backward rapidity. Decays of unstable particles are described by EVTGEN [65], and the interaction of the generated particles with the detector, and its response, are implemented using the GEANT4 toolkit [66,67] as described in Ref. [68]. A simulation sample is used for each collision configuration.

III. POLARIZATION MEASUREMENT

A. Signal selection and yields extraction

To reconstruct the Λ and $\bar{\Lambda}$ candidates, pairs of oppositely charged proton and pion candidates are selected and required to traverse all tracking detectors, have a good quality track fit, momentum greater than 5 GeV/c, and a common good-quality vertex. The particles must have a combined invariant mass $1100 < m(p\pi^-) < 1135\,\mathrm{MeV}/c^2$. Candidates are required to have a longitudinal position of the associated PV in the range $-180 < z_{\rm PV} < 180$ mm. A particle identification (PID) requirement based on a neural network trained to

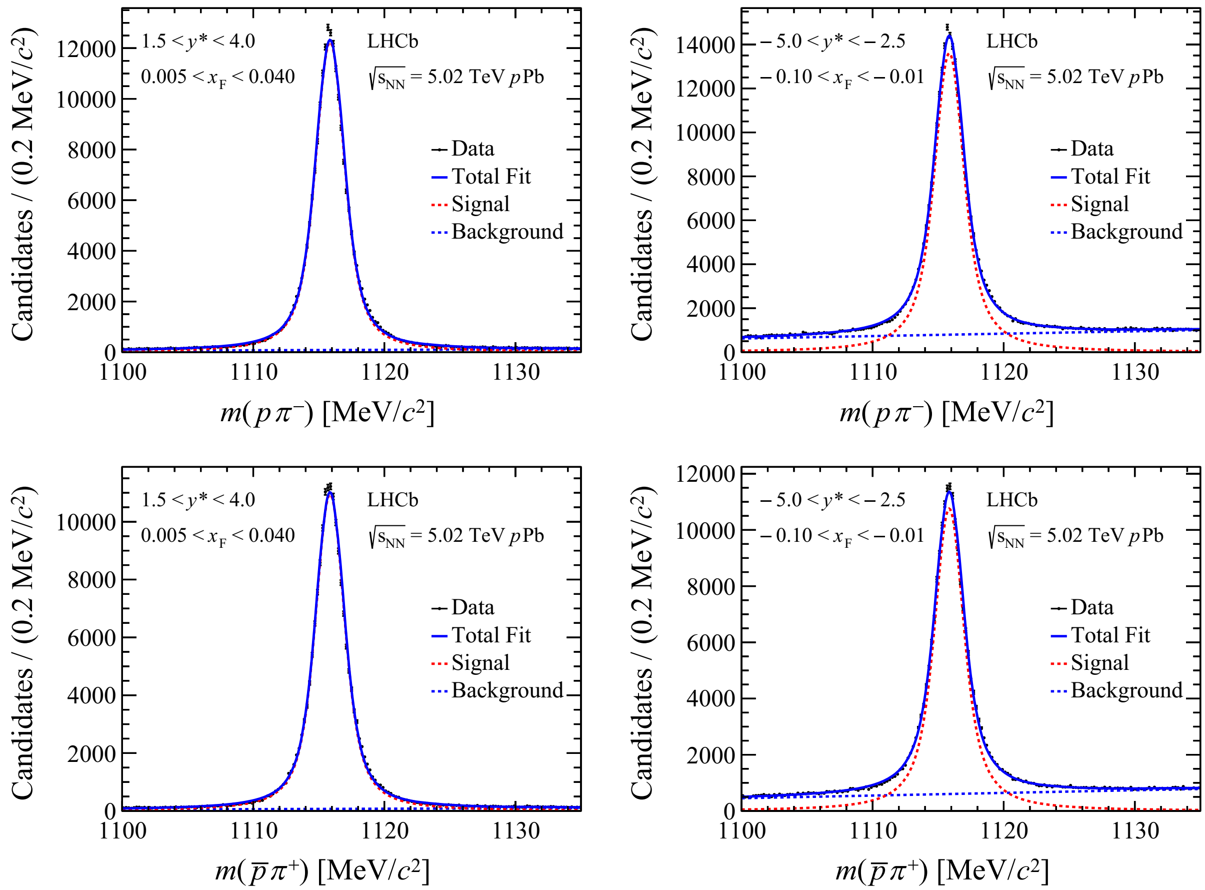

FIG. 1. Invariant-mass distribution for Λ (top) and $\bar{\Lambda}$ (bottom) candidates and fit results in data after all selection requirements for $0.15 < p_{\mathrm{T}} < 6.00\ \mathrm{GeV}/c$ in two intervals of y^* and x_{F}.

separate particle types using information from several detectors, including the RICH system, is applied to select protons. A discriminant, ν, is used to increase the signal-to-background ratio, following previous Λ production studies in LHCb [69]. The discriminant is based on the logarithm of the χ^2_{IP}, defined as the difference in the vertex-fit χ^2 of a given PV reconstructed with and without the particle under consideration. The variable is defined as $\nu = \log(I^+ I^- / I^0)$, where $I^\pm$ is the χ^2_{IP} of the proton or pion particle, and I^0 is the χ^2_{IP} of the Λ or $\bar{\Lambda}$ candidate. This requirement selects prompt contributions of Λ or $\bar{\Lambda}$ candidates produced directly in the collision as well as those from short-lived ($c\tau < 1$ nm) decays. With this selection and definition, the signal candidates are 98% prompt, which includes a 22% feed-down contribution from $\Sigma^0 \to \Lambda\gamma$ decays estimated from the EPOS-LHC simulation. According to the SU(6) quark model, the Σ^0 and Λ baryons are produced with opposite polarization orientations and differing polarization magnitudes following the relation $P_{\Sigma^0} = -\frac{1}{3} P_\Lambda$ [70–72], a relation that had also been predicted earlier in Ref. [73]. If the polarization of prompt Λ and Σ^0 baryons originate from the strange-quark spin, the feed-down contributions from $\Sigma^0 \to \Lambda\ \gamma$ decays are expected to reduce the magnitude of the observed Λ polarization.

The invariant-mass distributions for the selected Λ and $\bar{\Lambda}$ candidates are shown in Fig. 1. There are 231 358 (205 590) Λ ($\bar{\Lambda}$) and 396 045 (307 853) Λ ($\bar{\Lambda}$) candidates in the signal region, $1111 < m_{p\pi} < 1121\ \mathrm{MeV}/c^2$, at positive and negative y^*, respectively. The distributions are fitted using a binned, extended maximum-likelihood fit, where the signal component is modeled by a Voigtian function, a convolution of a Breit-Wigner with a Gaussian function. The mean, Breit-Wigner width, and Gaussian resolution are treated as free parameters, initialized to values estimated from simulation and constrained within bounds to ensure fit stability. Similarly, the background is modeled using a first-order Bernstein polynomial with two free parameters. Altogether, the fit includes seven free parameters: three for signal shape, two for background shape, and two for signal and background yields, all optimized simultaneously during the fit. The signal purity is about 97% and 85% in the signal region at positive and negative y^*, respectively, with the higher background at negative y^* due to the higher-multiplicity events when the lead beam enters the LHCb detector at the interaction point.

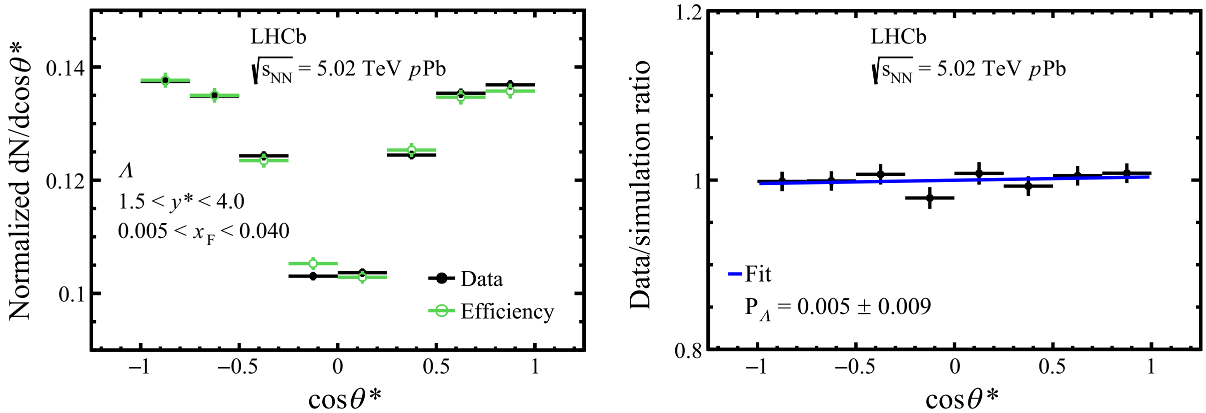

FIG. 2. Left: decay angle distribution measured in data and the total efficiency for Λ production in $1.5 < y^* < 4.0$ and $0.15 < p_T < 6.00$ GeV/c, where both have a common normalization. Right: corrected-data $\cos\theta^*$ distribution, along with the linear fit to extract the polarization. The fit reduced χ^2 is 4.2/6 and the error bars represent the sum in quadrature of the statistical uncertainties of data and simulation.

B. Efficiency determination

The total efficiency ε_{tot} in Eq. (1) includes the effects of geometric acceptance, the reconstruction and selection, and the PID criteria. The (anti)baryons generated in the EPOS-LHC simulated sample are unpolarized and, therefore, correspond to a uniform $\cos\theta^*$ distribution, which is affected by the detector acceptance and selection criteria. The signal yields in the simulated sample are derived from reconstructed candidates that are matched to generated (truth-level) particles following a standard matching algorithm. The simulation is adjusted using weights to improve agreement with data. The weight is calculated as the ratio of the normalized distributions of background-subtracted data and simulated signal in two-dimensional bins of p_T and η for the Λ and $\bar{\Lambda}$ baryons, and the independent variable z_{PV}. The weighting procedure has no impact on the $\cos\theta^*$ distribution. The PID efficiency is estimated in both simulation and data and computed as a function of p_T and η of the Λ and $\bar{\Lambda}$. The ratio of the efficiencies is applied as a weight to the simulation. The track-reconstruction efficiency from the simulation is corrected with a tag-and-probe method applied to data in two-dimensional intervals of η and p_T using a calibration sample of $J/\psi \to \mu^+\mu^-$ decays in the range $5 < p < 200$ GeVc [74]. Figure 2 (left) shows the decay angle distribution for protons from Λ baryons measured in data, along with the respective total efficiencies for $1.5 < y^* < 4.0$ and $0.15 < p_T < 6.00$ GeV/c. Each point is obtained by extracting the signal yield in the given bin using an independent fit to the invariant-mass distribution. The efficiency-corrected angular distribution and the fit to a linear function, $p_0(1 + p_1 \cos\theta^*)$, where p_0 and p_1 are free parameters, and $P_\Lambda = p_1/\alpha_\Lambda$, are shown on the right.

C. Systematic uncertainties

Several sources of systematic uncertainty are considered, and evaluated as the difference in the extracted polarization between the baseline and various alternative approaches. The systematic uncertainties related to signal modeling are estimated by performing an alternative fit represented by a Voigtian combined with an additional Gaussian distribution which introduces another resolution term as a free parameter in the fit. The uncertainty from the background modeling is evaluated by replacing the Bernstein polynomial with a first-degree polynomial with two free parameters in the fit. The uncertainty from the calculation of the simulation weights is estimated by calculating the weights using all particle candidates after selection requirements, without subtracting the background. Additionally, the effect of detector occupancy is taken into account by applying a weight to the simulation according to the track multiplicity. The uncertainty associated with the estimation of PID efficiencies is evaluated using an alternative method, in which the PID efficiency is calculated as the single-track proton efficiency in bins of proton momentum and η. Since the angular efficiency is derived from truth-matched yields and is sensitive to reduced matching performance for lower-quality tracks, a correction is applied to account for reconstructed candidates in simulation that fail to match a generated particle. The truth-matching efficiency is defined as the ratio of matched to total signal yields in simulation, where the latter also includes a fitted unmatched component determined from the invariant-mass distribution.

The correction is applied in two-dimensional bins of the angular distribution with p_T and x_F, and the associated systematic uncertainty is taken as the difference in the polarization result with and without this correction. The

TABLE I. Systematic uncertainty contributions for the forward ($1.5 < y^* < 4.0$) and backward ($-5.0 < y^* < -2.5$) collision configurations. The numbers represent the absolute systematic uncertainties of the integrated polarization values.

	Systematic uncertainty			
	Forward		Backward	
Source	Λ	$\bar{\Lambda}$	Λ	$\bar{\Lambda}$
Signal model	0.000	0.000	0.001	0.000
Background model	0.003	0.001	0.003	0.001
Kinematic weights	0.000	0.000	0.005	0.002
Simulation size	0.005	0.005	0.004	0.005
PID efficiencies	0.002	0.002	0.005	0.001
Truth matching efficiency	0.002	0.002	0.001	0.001
Binning of $\cos\theta^*$ distribution	0.003	0.002	0.003	0.000
Selection requirement on ν	0.002	0.002	0.001	0.002
Multiplicity dependence	0.000	0.000	0.000	0.001
Total	0.007	0.006	0.009	0.006

impact of the binning choice for the angular distribution used in the fit is also considered by repeating the polarization measurement using five bins instead of eight. The impact of the selection of ν is studied by varying the selection criteria above and below the baseline value. An additional uncertainty on the efficiency determination arises from the size of the simulation sample and is calculated by varying the simulated distribution by its statistical uncertainty. Other sources of uncertainty, such as the uncertainty on α_Λ or $\alpha_{\bar{\Lambda}}$ and the precession of the Λ or $\bar{\Lambda}$ spin as it traverses the magnetic field, are also considered but found to be negligible. The track reconstruction efficiency has an uncertainty due to the size of the calibration samples and the modeling of hadron material interactions, and is also found to be negligible. The total bin-dependent systematic uncertainty is computed in quadrature in bins of x_F and p_T. The systematic uncertainties for the integrated polarization values are shown in Table I.

Cross-checks are performed to investigate potential biases in the measurement. The polarization of the K^0_S meson, a pseudoscalar with null polarization, is measured using the same method and found to be consistent with zero (0.000 ± 0.003 and 0.000 ± 0.002 for the forward [$1.5 < y^* < 4.0$] and backward [$-5.0 < y^* < -2.5$] collision configurations, where the uncertainties are statistical only). The polarization is additionally calculated separately for each magnet polarity before combining, and the results are found to be consistent. A potential nonlinearity of the angular distribution is also considered by adding a quadratic term to the fitting model, which would be sensitive to residual imperfections in the modeling of the efficiency. No significant bias is observed in these cross-checks.

TABLE II. Polarization measured in the integrated kinematic range and in x_F and p_T bins for Λ in the forward ($1.5 < y^* < 4.0$) configuration.

Forward Λ	$\langle x_F \rangle$ (10^{-2})	$\langle p_T \rangle$ (GeV/c)	Polarization
Integrated	1.1	1.6	$0.005 \pm 0.008 \pm 0.007$
x_F ($\times 10^{-2}$)			
[0.5, 0.8]	0.7	1.3	$-0.010 \pm 0.016 \pm 0.013$
[0.8, 1.0]	0.9	1.5	$0.012 \pm 0.016 \pm 0.011$
[1.0, 2.0]	1.3	1.8	$0.012 \pm 0.012 \pm 0.008$
[2.0, 4.0]	2.4	2.8	$-0.018 \pm 0.040 \pm 0.036$
p_T (GeV/c)			
[0.15, 1.00]	0.8	0.8	$0.036 \pm 0.019 \pm 0.021$
[1.00, 1.50]	0.9	1.2	$-0.016 \pm 0.015 \pm 0.020$
[1.50, 2.00]	1.1	1.7	$-0.007 \pm 0.017 \pm 0.018$
[2.00, 2.50]	1.3	2.2	$0.028 \pm 0.022 \pm 0.017$
[2.50, 3.00]	1.4	2.7	$0.027 \pm 0.034 \pm 0.020$
[3.00, 4.00]	1.5	3.4	$-0.006 \pm 0.036 \pm 0.030$
[4.00, 6.00]	1.6	4.6	$0.049 \pm 0.066 \pm 0.049$

IV. RESULTS

The transverse polarization is determined by fitting the efficiency-corrected decay angle distribution based on Eq. (1). The polarization is measured for $0.15 < p_T < 6.00$ GeV/c, as well as for $0.005 < x_F < 0.040$ in the forward ($1.5 < y^* < 4.0$) configuration and $-0.10 < x_F < -0.01$ in the backward ($-5.0 < y^* < -2.5$) configuration. Figure 2 (right) shows the $\cos\theta^*$ distribution after

TABLE III. Polarization measured in the integrated kinematic range and in x_F and p_T bins for $\bar{\Lambda}$ in the forward ($1.5 < y^* < 4.0$) configuration.

Forward $\bar{\Lambda}$	$\langle x_F \rangle$ (10^{-2})	$\langle p_T \rangle$ (GeV/c)	Polarization
Integrated	1.0	1.6	$0.007 \pm 0.009 \pm 0.006$
x_F ($\times 10^{-2}$)			
[0.5, 0.8]	0.7	1.3	$-0.035 \pm 0.019 \pm 0.014$
[0.8, 1.0]	0.9	1.5	$0.028 \pm 0.019 \pm 0.012$
[1.0, 2.0]	1.3	1.8	$0.018 \pm 0.013 \pm 0.013$
[2.0, 4.0]	2.4	2.8	$-0.016 \pm 0.049 \pm 0.038$
p_T (GeV/c)			
[0.15, 1.00]	0.8	0.8	$-0.024 \pm 0.021 \pm 0.020$
[1.00, 1.50]	0.9	1.2	$0.013 \pm 0.015 \pm 0.018$
[1.50, 2.00]	1.1	1.7	$0.011 \pm 0.017 \pm 0.019$
[2.00, 2.50]	1.2	2.2	$0.008 \pm 0.024 \pm 0.017$
[2.50, 3.00]	1.4	2.7	$0.010 \pm 0.034 \pm 0.025$
[3.00, 4.00]	1.5	3.4	$0.031 \pm 0.040 \pm 0.030$
[4.00, 6.00]	1.6	4.6	$-0.006 \pm 0.068 \pm 0.039$

TABLE IV. Polarization measured in the integrated kinematic range and in x_F and p_T bins for Λ in the backward ($-5.0 < y^* < -2.5$) configuration.

Backward Λ	$\langle x_F \rangle$ (10^{-2})	$\langle p_T \rangle$ (GeV/c)	Polarization
Integrated	−2.7	1.6	$0.004 \pm 0.008 \pm 0.009$
x_F ($\times 10^{-2}$)			
[−10.0, −5.5]	−6.5	2.8	$-0.044 \pm 0.042 \pm 0.050$
[−5.5, −3.0]	−3.8	1.9	$0.004 \pm 0.013 \pm 0.018$
[−3.0, −2.0]	−2.4	1.5	$0.000 \pm 0.012 \pm 0.013$
[−2.0, −1.0]	−1.7	1.3	$0.016 \pm 0.018 \pm 0.025$
p_T (GeV/c)			
[0.15, 1.00]	−2.1	0.8	$0.045 \pm 0.021 \pm 0.020$
[1.00, 1.50]	−2.5	1.2	$0.001 \pm 0.013 \pm 0.016$
[1.50, 2.00]	−2.9	1.7	$-0.012 \pm 0.015 \pm 0.015$
[2.00, 2.50]	−3.4	2.2	$-0.019 \pm 0.020 \pm 0.015$
[2.50, 3.00]	−3.7	2.7	$-0.024 \pm 0.028 \pm 0.019$
[3.00, 4.00]	−4.0	3.4	$0.024 \pm 0.034 \pm 0.033$
[4.00, 6.00]	−4.3	4.6	$-0.021 \pm 0.063 \pm 0.040$

acceptance corrections integrated over the entire kinematic range for Λ baryons in the forward configuration. The linear fit and the corresponding extracted polarization value are shown, where the error bars represent the sum in quadrature of the data and simulation statistical uncertainties. The integrated polarization measurements for $1.5 < y^* < 4.0$ are

$$P_\Lambda = 0.005 \pm 0.008 \pm 0.007,$$
$$P_{\bar{\Lambda}} = 0.007 \pm 0.009 \pm 0.006.$$

TABLE V. Polarization measured in the integrated kinematic range and in x_F and p_T bins for $\bar{\Lambda}$ in the backward ($-5.0 < y^* < -2.5$) configuration.

Backward $\bar{\Lambda}$	$\langle x_F \rangle$ (10^{-2})	$\langle p_T \rangle$ (GeV/c)	Polarization
Integrated	−2.7	1.5	$-0.005 \pm 0.008 \pm 0.006$
x_F ($\times 10^{-2}$)			
[−10.0, −5.5]	−6.4	2.8	$0.027 \pm 0.050 \pm 0.026$
[−5.5, −3.0]	−3.8	1.9	$0.002 \pm 0.015 \pm 0.017$
[−3.0, −2.0]	−2.4	1.5	$-0.009 \pm 0.013 \pm 0.011$
[−2.0, −1.0]	−1.7	1.3	$-0.009 \pm 0.019 \pm 0.026$
p_T (GeV/c)			
[0.15, 1.00]	−2.1	0.8	$-0.002 \pm 0.021 \pm 0.023$
[1.00, 1.50]	−2.4	1.2	$-0.023 \pm 0.014 \pm 0.013$
[1.50, 2.00]	−2.9	1.7	$-0.004 \pm 0.016 \pm 0.014$
[2.00, 2.50]	−3.3	2.2	$0.010 \pm 0.022 \pm 0.018$
[2.50, 3.00]	−3.5	2.7	$-0.006 \pm 0.031 \pm 0.018$
[3.00, 4.00]	−3.8	3.4	$0.082 \pm 0.037 \pm 0.019$
[4.00, 6.00]	−4.0	4.6	$-0.002 \pm 0.069 \pm 0.048$

The integrated polarization measurements for $-5.0 < y^* < -2.5$ are

$$P_\Lambda = 0.004 \pm 0.008 \pm 0.009,$$
$$P_{\bar{\Lambda}} = -0.005 \pm 0.008 \pm 0.006.$$

The polarization is also determined in bins of p_T and x_F. The results are summarized in Tables II–V, where the first uncertainties are statistical from data, and the second represent the systematic uncertainties added in quadrature. Figures 3 and 4 show the results as a function of x_F and p_T, respectively. The statistical and systematic uncertainties are added in quadrature to obtain the total uncertainty. All measured polarization values are consistent with zero.

Figure 5 (left) shows the transverse Λ polarization measured in pPb collisions at $\sqrt{s_{NN}} = 5.02$ TeV for positive and negative x_F, together with earlier results from fixed-target pNe collision measured by LHCb-System for Measuring the Overlap with Gas (SMOG) [61] and from other unpolarized pp and pA experiments, including the M2 beamline [7] and the E799 experiment [9] at Fermilab, NA48 [10] and ATLAS experiment at the CERN Large Hadron Collider [12], and HERA-B experiment at Deutsches Elektronen-Synchrotron (DESY) [11]. The results have been rescaled to the α_Λ value used in this analysis and, where necessary, the x_F values were converted from the laboratory frame to the center-of-mass. The compared data span a wide range of collision energies, from fixed-target experiments at 27 GeV up to LHC measurements of 68 GeV, 5 and 7 TeV, and include different collision systems (pp, pBe, pC, pNe, and pPb). The fixed-target experiments cover lower p_T ranges (0.3–2 GeV/c), while ATLAS and LHCb extend to higher p_T. The fixed-target results show negative polarization, reaching $P_\Lambda \approx -0.3$ for $x_F \gtrsim 0.2$ and decreasing in magnitude as x_F approaches zero. A comparison of E799 ($0.67 < p_T < 2.15$ GeV/c) and NA48 ($0.28 < p_T < 0.86$ GeV/c) at overlapping x_F indicates a possible p_T dependence of the polarization magnitude. The present pPb results show polarization consistent with zero ($|P_\Lambda| \leq 0.05$) over the measured x_F range and p_T interval of 0.15–6.00 GeV/c. Figure 5 (right) shows on a logarithmic x_F scale the same comparison with the backward-rapidity results transformed to positive x_F values using the relation $P(-x_F) = -P(x_F)$, which must hold for symmetric collision systems such as pp, to include also previous results. In the asymmetric pPb collisions, possible deviations from zero at low x_F could arise from differences in interactions in the target or other nuclear effects; however, the present results show no significant deviation from zero within the uncertainties. The present LHCb measurements reach an average p_T up to 4.6 GeV/c, entering a perturbative regime where additional theoretical tools can be applied.

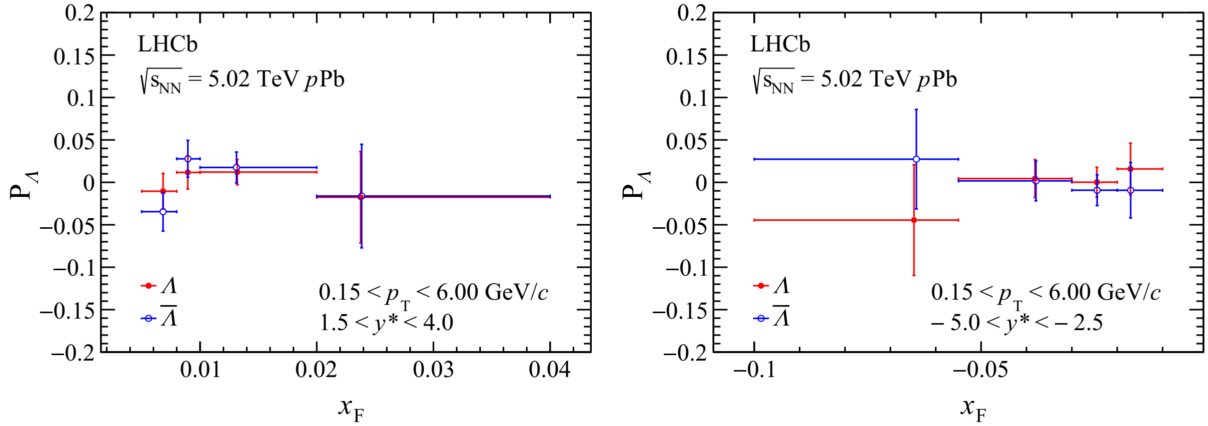

FIG. 3. Transverse polarization for Λ (red filled markers) and $\bar{\Lambda}$ (blue empty markers) baryons as a function of Feynman-x for (left) forward ($1.5 < y^* < 4.0$) and (right) backward ($-5.0 < y^* < -2.5$) collision configurations. The error bars represent the total uncertainty.

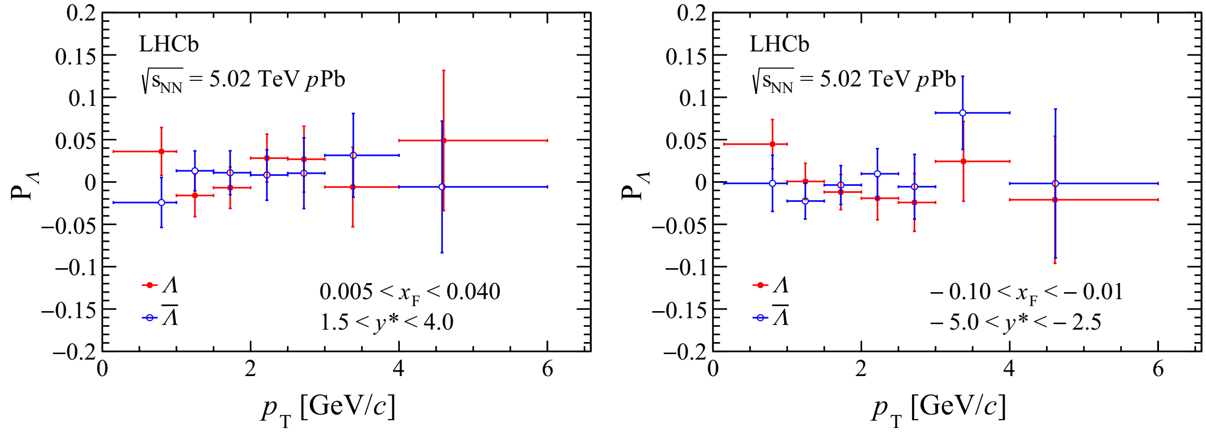

FIG. 4. Transverse polarization for Λ (red, filled) and $\bar{\Lambda}$ (blue, empty) as a function of transverse momentum for (left) forward and (right) backward collision configurations. The error bars represent the total uncertainty.

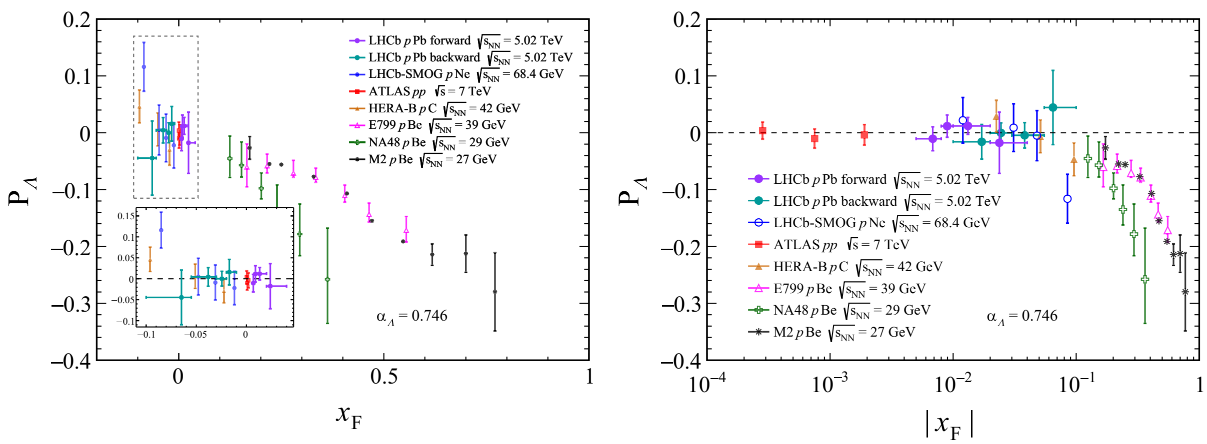

FIG. 5. Left: transverse Λ polarization measured in LHCb pPb collisions in the forward ($1.5 < y^* < 4.0$) and backward ($-5.0 < y^* < -2.5$) configurations and LHCb-SMOG fixed-target pNe collisions [61], compared with other measurements with different collision systems and different center-of-mass energies [7,9–12]. The values have been scaled to match the α_Λ value used in this paper. Right: transverse Λ polarization comparison with previous measurements, assuming the transformation $P(-x_F) = -P(x_F)$.

V. CONCLUSIONS

The Λ and $\bar{\Lambda}$ transverse polarization has been measured in pPb collisions at $\sqrt{s_{\mathrm{NN}}} = 5.02$ TeV as a function of p_{T} and x_{F}. The results are consistent with zero for both Λ and $\bar{\Lambda}$ in the forward and backward rapidity regions. This work expands the kinematic range of previous measurements, bridging the gap between midrapidity ATLAS measurements at low x_{F} [12] and other fixed-target measurements at high x_{F} with different collision energies and configurations [7,9,10,61]. The pPb results from LHCb agree with previous measurements, adding new data at different energy and collision configurations within a kinematic range that was previously underexplored. The p_{T} in this measurement extends to values higher than fixed-target experiments that have observed nonzero transverse Λ polarization. Compared with earlier observations of significant transverse Λ polarization in fixed-target data, the results presented in this paper indicate that the polarization effects are small towards low x_{F} at both positive and negative rapidity. These results contribute to ongoing efforts in understanding transverse spin effects in hadron collisions, providing constraints on the magnitude and kinematic dependence of fragmentation functions in a nuclear environment. In particular, they can offer input and tests for theoretical frameworks based on polarizing TMD FFs and multiparton correlators for the low-x_{F} region and asymmetric nuclear collisions.

ACKNOWLEDGMENTS

We express our gratitude to our colleagues in the CERN accelerator departments for the excellent performance of the LHC. We thank the technical and administrative staff at the LHCb institutes. We acknowledge support from CERN and from the national agencies: ARC (Australia); CAPES, CNPq, FAPERJ and FINEP (Brazil); MOST and NSFC (China); CNRS/IN2P3 (France); BMBF, DFG and MPG (Germany); INFN (Italy); NWO (Netherlands); MNiSW and NCN (Poland); MCID/IFA (Romania); MICIU and AEI (Spain); SNSF and SER (Switzerland); NASU (Ukraine); STFC (United Kingdom); DOE NP and NSF (USA). We acknowledge the computing resources that are provided by ARDC (Australia), CBPF (Brazil), CERN, IHEP and LZU (China), IN2P3 (France), KIT and DESY (Germany), INFN (Italy), SURF (Netherlands), Polish WLCG (Poland), IFIN-HH (Romania), PIC (Spain), CSCS (Switzerland), and GridPP (United Kingdom). We are indebted to the communities behind the multiple open-source software packages on which we depend. Individual groups or members have received support from Key Research Program of Frontier Sciences of CAS, CAS PIFI, CAS CCEPP, Fundamental Research Funds for the Central Universities, and Sci. & Tech. Program of Guangzhou (China); Minciencias (Colombia); EPLANET, Marie Skłodowska-Curie Actions, ERC and NextGenerationEU (European Union); A*MIDEX, ANR, IPhU and Labex P2IO, and Région Auvergne-Rhône-Alpes (France); Alexander-von-Humboldt Foundation (Germany); ICSC (Italy); Severo Ochoa and María de Maeztu Units of Excellence, GVA, XuntaGal, GENCAT, InTalent-Inditex and Prog. Atracción Talento CM (Spain); SRC (Sweden); the Leverhulme Trust, the Royal Society and UKRI (United Kingdom).

DATA AVAILABILITY

The data that support the findings of this article are openly available [75].

[1] G. Bunce *et al.*, Phys. Rev. Lett. **36**, 1113 (1976).
[2] K. J. Heller *et al.*, Phys. Rev. Lett. **41**, 607 (1978).
[3] G. L. Kane, J. Pumplin, and W. Repko, Phys. Rev. Lett. **41**, 1689 (1978).
[4] L. Schachinger *et al.*, Phys. Rev. Lett. **41**, 1348 (1978).
[5] S. Erhan *et al.*, Phys. Lett. **82B**, 301 (1979).
[6] K. J. Heller *et al.*, Phys. Rev. Lett. **51**, 2025 (1983).
[7] B. Lundberg *et al.*, Phys. Rev. D **40**, 3557 (1989).
[8] B. S. Yuldashev *et al.*, Phys. Rev. D **43**, 2792 (1991).
[9] E. J. Ramberg *et al.*, Phys. Lett. B **338**, 403 (1994).
[10] V. Fanti *et al.*, Eur. Phys. J. C **6**, 265 (1999).
[11] I. Abt *et al.* (HERA-B Collaboration), Phys. Lett. B **638**, 415 (2006).
[12] G. Aad *et al.* (ATLAS Collaboration), Phys. Rev. D **91**, 032004 (2015).
[13] P. H. Stuntebeck, N. M. Cason, J. M. Bishop, N. N. Biswas, V. P. Kenney, and W. D. Shephard, Phys. Rev. D **9**, 608 (1974).
[14] S. N. Ganguli *et al.* (Amsterdam-CERN-Nijmegen-Oxford Collaboration), Nuovo Cimento A **44**, 345 (1978).
[15] R. Sugahara *et al.*, Nucl. Phys. **B156**, 237 (1979).
[16] T. Haupt *et al.*, Z. Phys. C **28**, 57 (1985).
[17] S. A. Gourlay, H. L. Melanson, M. A. Abolins, K. W. Edwards, W. R. Francis, H. G. E. Kobrak, D. P. Owen, R. A. Swanson, and P. M. Yager, Phys. Rev. Lett. **56**, 2244 (1986).
[18] K. Ackerstaff *et al.* (OPAL Collaboration), Eur. Phys. J. C **2**, 49 (1998).
[19] P. Astier *et al.* (NOMAD Collaboration), Nucl. Phys. **B588**, 3 (2000).
[20] M. I. Adamovich *et al.* (WA89 Collaboration), Eur. Phys. J. C **32**, 221 (2004).

[21] J. L. Sanchez-Lopez *et al.* (SELEX Collaboration), arXiv:0706.3660.
[22] A. Airapetian *et al.* (HERMES Collaboration), Phys. Rev. D **76**, 092008 (2007).
[23] A. Airapetian *et al.* (HERMES Collaboration), Phys. Rev. D **90**, 072007 (2014).
[24] C. Bourrely, E. Leader, and J. Soffer, Phys. Rep. **59**, 95 (1980).
[25] L. G. Pondrom, Phys. Rep. **122**, 57 (1985).
[26] K. J. Heller, Conf. Proc. C **960910**, 23 (1996).
[27] A. D. Panagiotou, Int. J. Mod. Phys. A **05**, 1197 (1990).
[28] W. G. D. Dharmaratna and G. R. Goldstein, Phys. Rev. D **53**, 1073 (1996).
[29] M. Anselmino, D. Boer, U. D'Alesio, and F. Murgia, Phys. Rev. D **63**, 054029 (2001).
[30] D. Boer, in *17th International Workshop on Deep-Inelastic Scattering and Related Subjects* (2009), p. 199, arXiv:0907.1610.
[31] D. Boer, Z.-B. Kang, W. Vogelsang, and F. Yuan, Phys. Rev. Lett. **105**, 202001 (2010).
[32] L. Gamberg, Z.-B. Kang, D. Y. Shao, J. Terry, and F. Zhao, Phys. Lett. B **818**, 136371 (2021).
[33] Z.-B. Kang, J. Terry, A. Vossen, Q. Xu, and J. Zhang, Phys. Rev. D **105**, 094033 (2022).
[34] Y. Guan *et al.* (Belle Collaboration), Phys. Rev. Lett. **122**, 042001 (2019).
[35] M. Ablikim *et al.* (BESIII Collaboration), Nat. Phys. **15**, 631 (2019).
[36] J. Duryea *et al.*, Phys. Rev. Lett. **67**, 1193 (1991).
[37] C. Wilkinson *et al.*, Phys. Rev. Lett. **46**, 803 (1981).
[38] Y. W. Wah, T. R. Cardello, P. S. Cooper, L. J. Teig, J. L. Thron, C. Ankenbrandt, J. P. Berge, A. E. Brenner, J. Butler, K. Doroba, J. Lach, P. Laurikainen, J. Marriner, E. McCliment, E. W. Anderson, and A. Breakstone, Phys. Rev. Lett. **55**, 2551 (1985).
[39] E. C. Dukes *et al.*, Phys. Lett. B **193**, 135 (1987).
[40] K. B. Luk *et al.*, Phys. Rev. Lett. **70**, 900 (1993).
[41] P. M. Ho *et al.*, Phys. Rev. D **44**, 3402 (1991).
[42] A. Morelos Pineda *et al.* (E761 Collaboration), Phys. Rev. Lett. **71**, 2172 (1993).
[43] J. Collins, *Foundations of Perturbative QCD* (Cambridge University Press, Cambridge, England, 2011), Vol. 32.
[44] P. J. Mulders and R. D. Tangerman, Nucl. Phys. **B461**, 197 (1996).
[45] U. D'Alesio, F. Murgia, and M. Zaccheddu, Phys. Rev. D **102**, 054001 (2020).
[46] D. Callos, Z.-B. Kang, and J. Terry, Phys. Rev. D **102**, 096007 (2020).
[47] K.-B. Chen, Z.-T. Liang, Y.-L. Pan, Y.-K. Song, and S.-Y. Wei, Phys. Lett. B **816**, 136217 (2021).
[48] T. Gao (STAR Collaboration), Proc. Sci., SPIN2023 (**2024**) 031 [arXiv:2402.01168].
[49] Z.-B. Kang, K. Lee, and F. Zhao, Phys. Lett. B **809**, 135756 (2020).
[50] D. Boer, C. J. Bomhof, D. S. Hwang, and P. J. Mulders, Phys. Lett. B **659**, 127 (2008).
[51] U. D'Alesio, L. Gamberg, F. Murgia, and M. Zaccheddu, Phys. Lett. B **851**, 138552 (2024).
[52] Y. Gao, K.-B. Chen, Y.-K. Song, and S.-Y. Wei, Phys. Lett. B **858**, 139026 (2024).
[53] A. Metz and A. Vossen, Prog. Part. Nucl. Phys. **91**, 136 (2016).
[54] Y. Kanazawa and Y. Koike, Phys. Rev. D **64**, 034019 (2001).
[55] J. Zhou, F. Yuan, and Z.-T. Liang, Phys. Rev. D **78**, 114008 (2008).
[56] Y. Koike, K. Yabe, and S. Yoshida, Phys. Rev. D **92**, 094011 (2015).
[57] Y. Koike, A. Metz, D. Pitonyak, K. Yabe, and S. Yoshida, Phys. Rev. D **95**, 114013 (2017).
[58] R. Ikarashi, Y. Koike, K. Yabe, and S. Yoshida, Phys. Rev. D **106**, 074006 (2022).
[59] M. Vesterinen (LHCb Collaboration), Considerations on the LHCb dipole magnet polarity reversal (2014), https://cds.cern.ch/record/1642153.
[60] S. Navas *et al.* (Particle Data Group), Phys. Rev. D **110**, 030001 (2024).
[61] R. Aaij *et al.* (LHCb Collaboration), J. High Energy Phys. 09 (2024) 082.
[62] A. A. Alves Jr. *et al.* (LHCb Collaboration), J. Instrum. **3**, S08005 (2008).
[63] R. Aaij *et al.* (LHCb Collaboration), Int. J. Mod. Phys. A **30**, 1530022 (2015).
[64] T. Pierog, I. Karpenko, J. M. Katzy, E. Yatsenko, and K. Werner, Phys. Rev. C **92**, 034906 (2015).
[65] D. J. Lange, Nucl. Instrum. Methods Phys. Res., Sect. A **462**, 152 (2001).
[66] S. Agostinelli *et al.* (Geant4 Collaboration), Nucl. Instrum. Methods Phys. Res., Sect. A **506**, 250 (2003).
[67] J. Allison, K. Amako, J. Apostolakis, H. Araujo, P. Dubois *et al.* (Geant4 Collaboration), IEEE Trans. Nucl. Sci. **53**, 270 (2006).
[68] M. Clemencic *et al.*, J. Phys. Conf. Ser. **331**, 032023 (2011).
[69] R. Aaij *et al.* (LHCb Collaboration), J. High Energy Phys. 08 (2011) 034.
[70] B. Andersson, G. Gustafson, and G. Ingelman, Phys. Lett. **85B**, 417 (1979).
[71] B. Andersson, G. Gustafson, G. Ingelman, and T. Sjostrand, Phys. Rep. **97**, 31 (1983).
[72] G. Gustafson and J. Hakkinen, Phys. Lett. B **303**, 350 (1993).
[73] M. H. Cha and J. Sucher, Phys. Rev. **140**, B668 (1965).
[74] R. Aaij *et al.* (LHCb Collaboration), J. Instrum. **10**, P02007 (2015).
[75] https://cds.cern.ch/record/2937485/.

R. Aaij,[38] A. S. W. Abdelmotteleb,[57] C. Abellan Beteta,[51] F. Abudinén,[57] T. Ackernley,[61] A. A. Adefisoye,[69] B. Adeva,[47] M. Adinolfi,[55] P. Adlarson,[84] C. Agapopoulou,[14] C. A. Aidala,[86] Z. Ajaltouni,[11] S. Akar,[11] K. Akiba,[38] P. Albicocco,[28] J. Albrecht,[19,b] F. Alessio,[49] Z. Aliouche,[63] P. Alvarez Cartelle,[56] R. Amalric,[16]

S. Amato,[3] J. L. Amey,[55] Y. Amhis,[14] L. An,[6] L. Anderlini,[27] M. Andersson,[51] A. Andreianov,[44]
P. Andreola,[51] M. Andreotti,[26] A. Anelli,[31,49,c] D. Ao,[7] F. Archilli,[37,d] Z Areg,[69] M. Argenton,[26]
S. Arguedas Cuendis,[9,49] A. Artamonov,[44] M. Artuso,[69] E. Aslanides,[13] R. Ataíde Da Silva,[50] M. Atzeni,[65]
B. Audurier,[12] D. Bacher,[64] I. Bachiller Perea,[50] S. Bachmann,[22] M. Bachmayer,[50] J. J. Back,[57]
P. Baladron Rodriguez,[47] V. Balagura,[15] A. Balboni,[26] W. Baldini,[26] L. Balzani,[19] H. Bao,[7]
J. Baptista de Souza Leite,[61] C. Barbero Pretel,[47,12] M. Barbetti,[27] I. R. Barbosa,[70] R. J. Barlow,[63]
M. Barnyakov,[25] S. Barsuk,[14] W. Barter,[59] J. Bartz,[69] S. Bashir,[40] B. Batsukh,[5] P. B. Battista,[14] A. Bay,[50]
A. Beck,[65] M. Becker,[19] F. Bedeschi,[35] I. B. Bediaga,[2] N. A. Behling,[19] S. Belin,[47] K. Belous,[44] I. Belov,[29]
I. Belyaev,[36] G. Benane,[13] G. Bencivenni,[28] E. Ben-Haim,[16] A. Berezhnoy,[44] R. Bernet,[51] S. Bernet Andres,[46]
A. Bertolin,[33] C. Betancourt,[51] F. Betti,[59] J. Bex,[56] Ia. Bezshyiko,[51] O. Bezshyyko,[85] J. Bhom,[41]
M. S. Bieker,[18] N. V. Biesuz,[26] P. Billoir,[16] A. Biolchini,[38] M. Birch,[62] F. C. R. Bishop,[10] A. Bitadze,[63]
A. Bizzeti,[27,e] T. Blake,[57] F. Blanc,[50] J. E. Blank,[19] S. Blusk,[69] V. Bocharnikov,[44] J. A. Boelhauve,[19]
O. Boente Garcia,[15] T. Boettcher,[68] A. Bohare,[59] A. Boldyrev,[44] C. S. Bolognani,[81] R. Bolzonella,[26]
R. B. Bonacci,[1] N. Bondar,[44,49] A. Bordelius,[49] F. Borgato,[33,49] S. Borghi,[63] M. Borsato,[31,c] J. T. Borsuk,[82]
E. Bottalico,[61] S. A. Bouchiba,[50] M. Bovill,[64] T. J. V. Bowcock,[61] A. Boyer,[49] C. Bozzi,[26] J. D. Brandenburg,[87]
A. Brea Rodriguez,[50] N. Breer,[19] J. Brodzicka,[41] A. Brossa Gonzalo,[47,a] J. Brown,[61] D. Brundu,[32]
E. Buchanan,[59] L. Buonincontri,[33,f] M. Burgos Marcos,[81] A. T. Burke,[63] C. Burr,[49] J. S. Butter,[56] J. Buytaert,[49]
W. Byczynski,[49] S. Cadeddu,[32] H. Cai,[74] A. Caillet,[16] R. Calabrese,[26,g] S. Calderon Ramirez,[9] L. Calefice,[45]
S. Cali,[28] M. Calvi,[31,c] M. Calvo Gomez,[46] P. Camargo Magalhaes,[2,h] J. I. Cambon Bouzas,[47] P. Campana,[28]
D. H. Campora Perez,[81] A. F. Campoverde Quezada,[7] S. Capelli,[31] L. Capriotti,[26] R. Caravaca-Mora,[9]
A. Carbone,[25,i] L. Carcedo Salgado,[47] R. Cardinale,[29,j] A. Cardini,[32] P. Carniti,[31] L. Carus,[22] A. Casais Vidal,[65]
R. Caspary,[22] G. Casse,[61] M. Cattaneo,[49] G. Cavallero,[26,49] V. Cavallini,[26,g] S. Celani,[22] S. Cesare,[30,k]
A. J. Chadwick,[61] I. Chahrour,[86] H. Chang,[4,l] M. Charles,[16] Ph. Charpentier,[49] E. Chatzianagnostou,[38]
M. Chefdeville,[10] C. Chen,[56] S. Chen,[5] Z. Chen,[7] A. Chernov,[41] S. Chernyshenko,[53] X. Chiotopoulos,[81]
V. Chobanova,[83] M. Chrzaszcz,[41] A. Chubykin,[44] V. Chulikov,[28,36] P. Ciambrone,[28] X. Cid Vidal,[47]
G. Ciezarek,[49] P. Cifra,[38] P. E. L. Clarke,[59] M. Clemencic,[49] H. V. Cliff,[56] J. Closier,[49] C. Cocha Toapaxi,[22]
V. Coco,[49] J. Cogan,[13] E. Cogneras,[11] L. Cojocariu,[43] S. Collaviti,[50] P. Collins,[49] T. Colombo,[49]
M. Colonna,[19] A. Comerma-Montells,[45] L. Congedo,[24] A. Contu,[32] N. Cooke,[60] C. Coronel,[66] I. Corredoira,[12]
A. Correia,[16] G. Corti,[49] J. Cottee Meldrum,[55] B. Couturier,[49] D. C. Craik,[51] M. Cruz Torres,[2,m]
E. Curras Rivera,[50] R. Currie,[59] C. L. Da Silva,[68] S. Dadabaev,[44] L. Dai,[71] X. Dai,[4] E. Dall'Occo,[49]
J. Dalseno,[83] C. D'Ambrosio,[62] J. Daniel,[11] P. d'Argent,[24] G. Darze,[3] A. Davidson,[57] J. E. Davies,[63]
O. De Aguiar Francisco,[63] C. De Angelis,[32,n] F. De Benedetti,[49] J. de Boer,[38] K. De Bruyn,[80] S. De Capua,[63]
M. De Cian,[63] U. De Freitas Carneiro Da Graca,[2,o] E. De Lucia,[28] J. M. De Miranda,[2] L. De Paula,[3]
M. De Serio,[24,p] P. De Simone,[28] F. De Vellis,[19] J. A. de Vries,[81] F. Debernardis,[24] D. Decamp,[10] S. Dekkers,[1]
L. Del Buono,[16] B. Delaney,[65] H.-P. Dembinski,[19] J. Deng,[8] V. Denysenko,[51] O. Deschamps,[11] F. Dettori,[32,n]
B. Dey,[78] P. Di Nezza,[28] I. Diachkov,[44] S. Didenko,[44] S. Ding,[69] Y. Ding,[50] L. Dittmann,[22] V. Dobishuk,[53]
A. D. Docheva,[60] C. Dong,[4,l] A. M. Donohoe,[23] F. Dordei,[32] A. C. dos Reis,[2] A. D. Dowling,[69] W. Duan,[72]
P. Duda,[82] M. W. Dudek,[41] L. Dufour,[49] V. Duk,[34] P. Durante,[49] M. M. Duras,[82] J. M. Durham,[68]
O. D. Durmus,[78] A. Dziurda,[41] A. Dzyuba,[44] S. Easo,[58] E. Eckstein,[18] U. Egede,[1] A. Egorychev,[44]
V. Egorychev,[44] S. Eisenhardt,[59] E. Ejopu,[63] L. Eklund,[84] M. Elashri,[66] J. Ellbracht,[19] S. Ely,[62] A. Ene,[43]
J. Eschle,[69] S. Esen,[22] T. Evans,[38] F. Fabiano,[32] S. Faghih,[66] L. N. Falcao,[2] B. Fang,[7] R. Fantechi,[35]
L. Fantini,[34,49,q] M. Faria,[50] K. Farmer,[59] D. Fazzini,[31,c] L. Felkowski,[82] M. Feng,[5,7] M. Feo,[19]
A. Fernandez Casani,[48] M. Fernandez Gomez,[47] A. D. Fernez,[67] F. Ferrari,[25,i] F. Ferreira Rodrigues,[3]
M. Ferrillo,[51] M. Ferro-Luzzi,[49] S. Filippov,[44] R. A. Fini,[24] M. Fiorini,[26,g] M. Firlej,[40] K. L. Fischer,[64]
D. S. Fitzgerald,[86] C. Fitzpatrick,[63] T. Fiutowski,[40] F. Fleuret,[15] A. Fomin,[52] M. Fontana,[25] L. F. Foreman,[63]
R. Forty,[49] D. Foulds-Holt,[59] V. Franco Lima,[3] M. Franco Sevilla,[67] M. Frank,[49] E. Franzoso,[26,g] G. Frau,[63]
C. Frei,[49] D. A. Friday,[63] J. Fu,[7] Q. Führing,[19,56,b] Y. Fujii,[1] T. Fulghesu,[13] E. Gabriel,[38] G. Galati,[24]
M. D. Galati,[38] A. Gallas Torreira,[47] D. Galli,[25,i] S. Gambetta,[59] M. Gandelman,[3] P. Gandini,[30] B. Ganie,[63]
H. Gao,[7] R. Gao,[64] T. Q. Gao,[56] Y. Gao,[8] Y. Gao,[6] Y. Gao,[8] L. M. Garcia Martin,[50] P. Garcia Moreno,[45]

J. García Pardiñas,[65] P. Gardner,[67] K. G. Garg,[8] L. Garrido,[45] C. Gaspar,[49] A. Gavrikov,[33] L. L. Gerken,[19] E. Gersabeck,[20] M. Gersabeck,[20] T. Gershon,[57] S. Ghizzo,[29,j] Z. Ghorbanimoghaddam,[55] L. Giambastiani,[33,f] F. I. Giasemis,[16,r] V. Gibson,[56] H. K. Giemza,[42] A. L. Gilman,[64] M. Giovannetti,[28] A. Gioventù,[45] L. Girardey,[63,58] M. A. Giza,[41] F. C. Glaser,[14,22] V. V. Gligorov,[16] C. Göbel,[70] L. Golinka-Bezshyyko,[85] E. Golobardes,[46] D. Golubkov,[44] A. Golutvin,[62,49] S. Gomez Fernandez,[45] W. Gomulka,[40] F. Goncalves Abrantes,[64] M. Goncerz,[41] G. Gong,[4,l] J. A. Gooding,[19] I. V. Gorelov,[44] C. Gotti,[31] E. Govorkova,[65] J. P. Grabowski,[18] L. A. Granado Cardoso,[49] E. Graugés,[45] E. Graverini,[50,s] L. Grazette,[57] G. Graziani,[27] A. T. Grecu,[43] L. M. Greeven,[38] N. A. Grieser,[66] L. Grillo,[60] S. Gromov,[44] C. Gu,[15] M. Guarise,[26] L. Guerry,[11] V. Guliaeva,[44] P. A. Günther,[22] A.-K. Guseinov,[50] E. Gushchin,[44] Y. Guz,[6,49] T. Gys,[49] K. Habermann,[18] T. Hadavizadeh,[1] C. Hadjivasiliou,[67] G. Haefeli,[50] C. Haen,[49] G. Hallett,[57] P. M. Hamilton,[67] J. Hammerich,[61] Q. Han,[33] X. Han,[22,49] S. Hansmann-Menzemer,[22] L. Hao,[7] N. Harnew,[64] T. H. Harris,[1] M. Hartmann,[14] S. Hashmi,[40] J. He,[7,t] F. Hemmer,[49] C. Henderson,[66] R. D. L. Henderson,[1] A. M. Hennequin,[49] K. Hennessy,[61] L. Henry,[50] J. Herd,[62] P. Herrero Gascon,[22] J. Heuel,[17] A. Hicheur,[3] G. Hijano Mendizabal,[51] J. Horswill,[63] R. Hou,[8] Y. Hou,[11] N. Howarth,[61] J. Hu,[72] W. Hu,[7] X. Hu,[4,l] W. Hulsbergen,[38] R. J. Hunter,[57] M. Hushchyn,[44] D. Hutchcroft,[61] M. Idzik,[40] D. Ilin,[44] P. Ilten,[66] A. Inglessi,[44] A. Iniukhin,[44] A. Ishteev,[44] K. Ivshin,[44] H. Jage,[17] S. J. Jaimes Elles,[76,48,49] S. Jakobsen,[49] E. Jans,[38] B. K. Jashal,[48] A. Jawahery,[67] V. Jevtic,[19] E. Jiang,[67] X. Jiang,[5,7] Y. Jiang,[7] Y. J. Jiang,[6] M. John,[64] A. John Rubesh Rajan,[23] D. Johnson,[54] C. R. Jones,[56] T. P. Jones,[57] S. Joshi,[42] B. Jost,[49] J. Juan Castella,[56] N. Jurik,[49] I. Juszczak,[41] D. Kaminaris,[50] S. Kandybei,[52] M. Kane,[59] Y. Kang,[4,l] C. Kar,[11] M. Karacson,[49] D. Karpenkov,[44] A. Kauniskangas,[50] J. W. Kautz,[66] M. K. Kazanecki,[41] F. Keizer,[49] M. Kenzie,[56] T. Ketel,[38] B. Khanji,[69] A. Kharisova,[44] S. Kholodenko,[35,49] G. Khreich,[14] T. Kirn,[17] V. S. Kirsebom,[31,c] O. Kitouni,[65] S. Klaver,[39] N. Kleijne,[35,u] K. Klimaszewski,[42] M. R. Kmiec,[42] S. Koliiev,[53] L. Kolk,[19] A. Konoplyannikov,[6] P. Kopciewicz,[49] P. Koppenburg,[38] A. Korchin,[52] M. Korolev,[44] I. Kostiuk,[38] O. Kot,[53] S. Kotriakhova, A. Kozachuk,[44] P. Kravchenko,[44] L. Kravchuk,[44] M. Kreps,[57] P. Krokovny,[44] W. Krupa,[69] W. Krzemien,[42] O. Kshyvanskyi,[53] S. Kubis,[82] M. Kucharczyk,[41] V. Kudryavtsev,[44] E. Kulikova,[44] A. Kupsc,[84] V. Kushnir,[52] B. Kutsenko,[13] I. Kyryllin,[52] D. Lacarrere,[49] P. Laguarta Gonzalez,[45] A. Lai,[32] A. Lampis,[32] D. Lancierini,[62] C. Landesa Gomez,[47] J. J. Lane,[1] G. Lanfranchi,[28] C. Langenbruch,[22] J. Langer,[19] O. Lantwin,[44] T. Latham,[57] F. Lazzari,[35,49,s] C. Lazzeroni,[54] R. Le Gac,[13] H. Lee,[61] R. Lefèvre,[11] A. Leflat,[44] S. Legotin,[44] M. Lehuraux,[57] E. Lemos Cid,[49] O. Leroy,[13] T. Lesiak,[41] E. D. Lesser,[49] B. Leverington,[22] A. Li,[4,l] C. Li,[4] C. Li,[13] H. Li,[72] J. Li,[8] K. Li,[75] L. Li,[63] M. Li,[8] P. Li,[7] P.-R. Li,[73] Q. Li,[5,7] S. Li,[8] T. Li,[71] T. Li,[72] Y. Li,[8] Y. Li,[5] Z. Lian,[4,l] X. Liang,[69] S. Libralon,[48] C. Lin,[7] T. Lin,[58] R. Lindner,[49] H. Linton,[62] R. Litvinov,[32,49] D. Liu,[8] F. L. Liu,[1] G. Liu,[72] K. Liu,[73] S. Liu,[5,7] W. Liu,[8] Y. Liu,[59] Y. Liu,[73] Y. L. Liu,[62] G. Loachamin Ordonez,[70] A. Lobo Salvia,[45] A. Loi,[32] T. Long,[56] J. H. Lopes,[3] A. Lopez Huertas,[45] S. López Soliño,[47] Q. Lu,[15] C. Lucarelli,[27,v] D. Lucchesi,[33,f] M. Lucio Martinez,[48] Y. Luo,[6] A. Lupato,[33,w] E. Luppi,[26,g] K. Lynch,[23] X.-R. Lyu,[7] G. M. Ma,[4,l] S. Maccolini,[19] F. Machefert,[14] F. Maciuc,[43] B. Mack,[69] I. Mackay,[64] L. M. Mackey,[69] L. R. Madhan Mohan,[56] M. J. Madurai,[54] D. Magdalinski,[38] D. Maisuzenko,[44] J. J. Malczewski,[41] S. Malde,[64] L. Malentacca,[49] A. Malinin,[44] T. Maltsev,[44] G. Manca,[32,n] G. Mancinelli,[13] C. Mancuso,[14] R. Manera Escalero,[45] F. M. Manganella,[37] D. Manuzzi,[25] D. Marangotto,[30] J. F. Marchand,[10] R. Marchevski,[50] U. Marconi,[25] E. Mariani,[16] S. Mariani,[49] C. Marin Benito,[45] J. Marks,[22] A. M. Marshall,[55] L. Martel,[64] G. Martelli,[34] G. Martellotti,[36] L. Martinazzoli,[49] M. Martinelli,[31,c] D. Martinez Gomez,[80] D. Martinez Santos,[83] F. Martinez Vidal,[48] A. Martorell i Granollers,[46] A. Massafferri,[2] R. Matev,[49] A. Mathad,[49] V. Matiunin,[44] C. Matteuzzi,[69] K. R. Mattioli,[15] A. Mauri,[62] E. Maurice,[15] J. Mauricio,[45] P. Mayencourt,[50] J. Mazorra de Cos,[48] M. Mazurek,[42] M. McCann,[62] T. H. McGrath,[63] N. T. McHugh,[60] A. McNab,[63] R. McNulty,[23] B. Meadows,[66] G. Meier,[19] D. Melnychuk,[42] F. M. Meng,[4,l] M. Merk,[38,81] A. Merli,[50] L. Meyer Garcia,[67] D. Miao,[5,7] H. Miao,[7] M. Mikhasenko,[77] D. A. Milanes,[76,x] A. Minotti,[31,c] E. Minucci,[28] T. Miralles,[11] B. Mitreska,[19] D. S. Mitzel,[19] A. Modak,[58] L. Moeser,[19] R. A. Mohammed,[64] R. D. Moise,[17] E. F. Molina Cardenas,[86] T. Mombächer,[49] M. Monk,[57,1] S. Monteil,[11] A. Morcillo Gomez,[47] G. Morello,[28] M. J. Morello,[35,u] M. P. Morgenthaler,[22] J. Moron,[40] W. Morren,[38] A. B. Morris,[49] A. G. Morris,[13] R. Mountain,[69] H. Mu,[4,l] Z. M. Mu,[6] E. Muhammad,[57] F. Muheim,[59] M. Mulder,[80] K. Müller,[51]

F. Muñoz-Rojas,[9] R. Murta,[62] V. Mytrochenko,[52] P. Naik,[61] T. Nakada,[50] R. Nandakumar,[58] T. Nanut,[49] I. Nasteva,[3] M. Needham,[59] E. Nekrasova,[44] N. Neri,[30,k] S. Neubert,[18] N. Neufeld,[49] P. Neustroev,[44] J. Nicolini,[49] D. Nicotra,[81] E. M. Niel,[15] N. Nikitin,[44] Q. Niu,[73] P. Nogarolli,[3] P. Nogga,[18] C. Normand,[55] J. Novoa Fernandez,[47] G. Nowak,[66] C. Nunez,[86] H. N. Nur,[60] A. Oblakowska-Mucha,[40] V. Obraztsov,[44] T. Oeser,[17] S. Okamura,[26,g] A. Okhotnikov,[44] O. Okhrimenko,[53] R. Oldeman,[32,n] F. Oliva,[59] M. Olocco,[19] C. J. G. Onderwater,[81] R. H. O'Neil,[49] D. Osthues,[19] J. M. Otalora Goicochea,[3] P. Owen,[51] A. Oyanguren,[48] O. Ozcelik,[59] F. Paciolla,[35,y] A. Padee,[42] K. O. Padeken,[18] B. Pagare,[47] T. Pajero,[49] A. Palano,[24] M. Palutan,[28] X. Pan,[4,l] S. Panebianco,[12] G. Panshin,[5] L. Paolucci,[57] A. Papanestis,[58,49] M. Pappagallo,[24,p] L. L. Pappalardo,[26] C. Pappenheimer,[66] C. Parkes,[63] D. Parmar,[77] B. Passalacqua,[26,g] G. Passaleva,[27] D. Passaro,[35,49,u] A. Pastore,[24] M. Patel,[62] J. Patoc,[64] C. Patrignani,[25,i] A. Paul,[69] C. J. Pawley,[81] A. Pellegrino,[38] J. Peng,[5,7] M. Pepe Altarelli,[28] S. Perazzini,[25] D. Pereima,[44] H. Pereira Da Costa,[68] A. Pereiro Castro,[47] P. Perret,[11] A. Perrevoort,[80] A. Perro,[49,13] M. J. Peters,[66] K. Petridis,[55] A. Petrolini,[29,j] J. P. Pfaller,[66] H. Pham,[69] L. Pica,[35,u] M. Piccini,[34] L. Piccolo,[32] B. Pietrzyk,[10] G. Pietrzyk,[14] R. N. Pilato,[61] D. Pinci,[36] F. Pisani,[49] M. Pizzichemi,[31,49,c] V. M. Placinta,[43] M. Plo Casasus,[47] T. Poeschl,[49] F. Polci,[16] M. Poli Lener,[28] A. Poluektov,[13] N. Polukhina,[44] I. Polyakov,[63] E. Polycarpo,[3] S. Ponce,[49] D. Popov,[7,49] S. Poslavskii,[44] K. Prasanth,[59] C. Prouve,[83] D. Provenzano,[32,n] V. Pugatch,[53] G. Punzi,[35,s] S. Qasim,[51] Q. Q. Qian,[6] W. Qian,[7] N. Qin,[4,l] S. Qu,[4,l] R. Quagliani,[49] R. I. Rabadan Trejo,[57] J. H. Rademacker,[55] M. Rama,[35] M. Ramírez García,[86] V. Ramos De Oliveira,[70] M. Ramos Pernas,[57] M. S. Rangel,[3] F. Ratnikov,[44] G. Raven,[39] M. Rebollo De Miguel,[48] F. Redi,[30,w] J. Reich,[55] F. Reiss,[20] Z. Ren,[7] P. K. Resmi,[64] M. Ribalda Galvez,[45] R. Ribatti,[50] G. Ricart,[15,12] D. Riccardi,[35,u] S. Ricciardi,[58] K. Richardson,[65] M. Richardson-Slipper,[59] K. Rinnert,[61] P. Robbe,[14,49] G. Robertson,[60] E. Rodrigues,[61] A. Rodriguez Alvarez,[45] E. Rodriguez Fernandez,[47] J. A. Rodriguez Lopez,[76] E. Rodriguez Rodriguez,[49] J. Roensch,[19] A. Rogachev,[44] A. Rogovskiy,[58] D. L. Rolf,[19] P. Roloff,[49] V. Romanovskiy,[66] A. Romero Vidal,[47] G. Romolini,[26] F. Ronchetti,[50] T. Rong,[6] M. Rotondo,[28] S. R. Roy,[22] M. S. Rudolph,[69] M. Ruiz Diaz,[22] R. A. Ruiz Fernandez,[47] J. Ruiz Vidal,[81] J. J. Saavedra-Arias,[9] J. J. Saborido Silva,[47] R. Sadek,[15] N. Sagidova,[44] D. Sahoo,[78] N. Sahoo,[54] B. Saitta,[32,n] M. Salomoni,[31,49,c] I. Sanderswood,[48] R. Santacesaria,[36] C. Santamarina Rios,[47] M. Santimaria,[28] L. Santoro,[2] E. Santovetti,[37] A. Saputi,[26,49] D. Saranin,[44] A. Sarnatskiy,[80] G. Sarpis,[59] M. Sarpis,[79] C. Satriano,[36,z] A. Satta,[37] M. Saur,[73] D. Savrina,[44] H. Sazak,[17] F. Sborzacchi,[49,28] A. Scarabotto,[19] S. Schael,[17] S. Scherl,[61] M. Schiller,[22] H. Schindler,[49] M. Schmelling,[21] B. Schmidt,[49] S. Schmitt,[17] H. Schmitz,[18] O. Schneider,[50] A. Schopper,[62] N. Schulte,[19] S. Schulte,[50] M. H. Schune,[14] G. Schwering,[17] B. Sciascia,[28] A. Sciuccati,[49] I. Segal,[77] S. Sellam,[47] A. Semennikov,[44] T. Senger,[51] M. Senghi Soares,[39] A. Sergi,[29,j] N. Serra,[51] L. Sestini,[27] A. Seuthe,[19] B. Sevilla Sanjuan,[46] Y. Shang,[6] D. M. Shangase,[86] M. Shapkin,[44] R. S. Sharma,[69] I. Shchemerov,[44] L. Shchutska,[50] T. Shears,[61] L. Shekhtman,[44] Z. Shen,[38] S. Sheng,[5,7] V. Shevchenko,[44] B. Shi,[7] Q. Shi,[7] Y. Shimizu,[14] E. Shmanin,[25] R. Shorkin,[44] J. D. Shupperd,[69] R. Silva Coutinho,[69] G. Simi,[33,f] S. Simone,[24,p] M. Singha,[78] N. Skidmore,[57] T. Skwarnicki,[69] M. W. Slater,[54] E. Smith,[65] K. Smith,[68] M. Smith,[62] L. Soares Lavra,[59] M. D. Sokoloff,[66] F. J. P. Soler,[60] A. Solomin,[55] A. Solovev,[44] I. Solovyev,[44] N. S. Sommerfeld,[18] R. Song,[1] Y. Song,[50] Y. Song,[4,l] Y. S. Song,[6] F. L. Souza De Almeida,[69] B. Souza De Paula,[3] E. Spadaro Norella,[29,j] E. Spedicato,[25] J. G. Speer,[19] E. Spiridenkov,[44] P. Spradlin,[60] V. Sriskaran,[49] F. Stagni,[49] M. Stahl,[77] S. Stahl,[49] S. Stanislaus,[64] M. Stefaniak,[87] E. N. Stein,[49] O. Steinkamp,[51] O. Stenyakin,[44] H. Stevens,[19] D. Strekalina,[44] Y. Su,[7] F. Suljik,[64] J. Sun,[32] L. Sun,[74] D. Sundfeld,[2] W. Sutcliffe,[51] K. Swientek,[40] F. Swystun,[56] A. Szabelski,[42] T. Szumlak,[40] Y. Tan,[4,l] Y. Tang,[74] Y. T. Tang,[7] M. D. Tat,[22] A. Terentev,[44] F. Terzuoli,[35,49,y] F. Teubert,[49] E. Thomas,[49] D. J. D. Thompson,[54] H. Tilquin,[62] V. Tisserand,[11] S. T'Jampens,[10] M. Tobin,[5] L. Tomassetti,[26,g] G. Tonani,[30] X. Tong,[6] T. Tork,[30] D. Torres Machado,[2] L. Toscano,[19] D. Y. Tou,[4,l] C. Trippl,[46] G. Tuci,[22] N. Tuning,[38] L. H. Uecker,[22] A. Ukleja,[40] D. J. Unverzagt,[22] A. Upadhyay,[49] B. Urbach,[59] A. Usachov,[39] A. Ustyuzhanin,[44] U. Uwer,[22] V. Vagnoni,[25] V. Valcarce Cadenas,[47] G. Valenti,[25] N. Valls Canudas,[49] J. van Eldik,[49] H. Van Hecke,[68] E. van Herwijnen,[62] C. B. Van Hulse,[47,aa] R. Van Laak,[50] M. van Veghel,[38] G. Vasquez,[51] R. Vazquez Gomez,[45] P. Vazquez Regueiro,[47] C. Vázquez Sierra,[83] S. Vecchi,[26] J. J. Velthuis,[55] M. Veltri,[27,bb] A. Venkateswaran,[50] M. Verdoglia,[32] M. Vesterinen,[57] D. Vico Benet,[64] P. Vidrier Villalba,[45] M. Vieites Diaz,[47] X. Vilasis-Cardona,[46]

E. Vilella Figueras,[61] A. Villa,[25] P. Vincent,[16] B. Vivacqua,[3] F. C. Volle,[54] D. vom Bruch,[13] N. Voropaev,[44] K. Vos,[81] C. Vrahas,[59] J. Wagner,[19] J. Walsh,[35] E. J. Walton,[1,57] G. Wan,[6] A. Wang,[7] C. Wang,[22] G. Wang,[8] H. Wang,[73] J. Wang,[6] J. Wang,[5] J. Wang,[4,l] J. Wang,[74] M. Wang,[49] N. W. Wang,[7] R. Wang,[55] X. Wang,[8] X. Wang,[72] X. W. Wang,[62] Y. Wang,[75] Y. Wang,[6] Y. H. Wang,[73] Z. Wang,[14] Z. Wang,[4,l] Z. Wang,[30] J. A. Ward,[57,1] M. Waterlaat,[49] N. K. Watson,[54] D. Websdale,[62] Y. Wei,[6] J. Wendel,[83] B. D. C. Westhenry,[55] C. White,[56] M. Whitehead,[60] E. Whiter,[54] A. R. Wiederhold,[63] D. Wiedner,[19] G. Wilkinson,[64,49] M. K. Wilkinson,[66] M. Williams,[65] M. J. Williams,[49] M. R. J. Williams,[59] R. Williams,[56] Z. Williams,[55] F. F. Wilson,[58] M. Winn,[12] W. Wislicki,[42] M. Witek,[41] L. Witola,[19] G. Wormser,[14] S. A. Wotton,[56] H. Wu,[69] J. Wu,[8] X. Wu,[74] Y. Wu,[6,56] Z. Wu,[7] K. Wyllie,[49] S. Xian,[72] Z. Xiang,[5] Y. Xie,[8] T. X. Xing,[30] A. Xu,[35,u] L. Xu,[4,l] L. Xu,[4,l] M. Xu,[49] Z. Xu,[49] Z. Xu,[7] Z. Xu,[5] K. Yang,[62] X. Yang,[6] Y. Yang,[29] Z. Yang,[6] V. Yeroshenko,[14] H. Yeung,[63] H. Yin,[8] X. Yin,[7] C. Y. Yu,[6] J. Yu,[71] X. Yuan,[5] Y Yuan,[5,7] E. Zaffaroni,[50] M. Zavertyaev,[21] M. Zdybal,[41] F. Zenesini,[25] C. Zeng,[5,7] M. Zeng,[4,l] C. Zhang,[6] D. Zhang,[8] J. Zhang,[7] L. Zhang,[4,l] R. Zhang,[8] S. Zhang,[71] S. Zhang,[64] Y. Zhang,[6] Y. Z. Zhang,[4,l] Z. Zhang,[4,l] Y. Zhao,[22] A. Zhelezov,[22] S. Z. Zheng,[6] X. Z. Zheng,[4,l] Y. Zheng,[7] T. Zhou,[6] X. Zhou,[8] Y. Zhou,[7] V. Zhovkovska,[57] L. Z. Zhu,[7] X. Zhu,[4,l] X. Zhu,[8] Y. Zhu,[17] V. Zhukov,[17] J. Zhuo,[48] Q. Zou,[5,7] D. Zuliani,[33,f] and G. Zunica[50]

(LHCb Collaboration)

[1]*School of Physics and Astronomy, Monash University, Melbourne, Australia*
[2]*Centro Brasileiro de Pesquisas Físicas (CBPF), Rio de Janeiro, Brazil*
[3]*Universidade Federal do Rio de Janeiro (UFRJ), Rio de Janeiro, Brazil*
[4]*Department of Engineering Physics, Tsinghua University, Beijing, China*
[5]*Institute Of High Energy Physics (IHEP), Beijing, China*
[6]*School of Physics State Key Laboratory of Nuclear Physics and Technology, Peking University, Beijing, China*
[7]*University of Chinese Academy of Sciences, Beijing, China*
[8]*Institute of Particle Physics, Central China Normal University, Wuhan, Hubei, China*
[9]*Consejo Nacional de Rectores (CONARE), San Jose, Costa Rica*
[10]*Université Savoie Mont Blanc, CNRS, IN2P3-LAPP, Annecy, France*
[11]*Université Clermont Auvergne, CNRS/IN2P3, LPC, Clermont-Ferrand, France*
[12]*Université Paris-Saclay, Centre d'Etudes de Saclay (CEA), IRFU, Saclay, France, Gif-Sur-Yvette, France*
[13]*Aix Marseille Univ, CNRS/IN2P3, CPPM, Marseille, France*
[14]*Université Paris-Saclay, CNRS/IN2P3, IJCLab, Orsay, France*
[15]*Laboratoire Leprince-Ringuet, CNRS/IN2P3, Ecole Polytechnique, Institut Polytechnique de Paris, Palaiseau, France*
[16]*LPNHE, Sorbonne Université, Paris Diderot Sorbonne Paris Cité, CNRS/IN2P3, Paris, France*
[17]*I. Physikalisches Institut, RWTH Aachen University, Aachen, Germany*
[18]*Universität Bonn - Helmholtz-Institut für Strahlen und Kernphysik, Bonn, Germany*
[19]*Fakultät Physik, Technische Universität Dortmund, Dortmund, Germany*
[20]*Physikalisches Institut, Albert-Ludwigs-Universität Freiburg, Freiburg, Germany*
[21]*Max-Planck-Institut für Kernphysik (MPIK), Heidelberg, Germany*
[22]*Physikalisches Institut, Ruprecht-Karls-Universität Heidelberg, Heidelberg, Germany*
[23]*School of Physics, University College Dublin, Dublin, Ireland*
[24]*INFN Sezione di Bari, Bari, Italy*
[25]*INFN Sezione di Bologna, Bologna, Italy*
[26]*INFN Sezione di Ferrara, Ferrara, Italy*
[27]*INFN Sezione di Firenze, Firenze, Italy*
[28]*INFN Laboratori Nazionali di Frascati, Frascati, Italy*
[29]*INFN Sezione di Genova, Genova, Italy*
[30]*INFN Sezione di Milano, Milano, Italy*
[31]*INFN Sezione di Milano-Bicocca, Milano, Italy*
[32]*INFN Sezione di Cagliari, Monserrato, Italy*
[33]*INFN Sezione di Padova, Padova, Italy*
[34]*INFN Sezione di Perugia, Perugia, Italy*
[35]*INFN Sezione di Pisa, Pisa, Italy*

[36]INFN Sezione di Roma La Sapienza, Roma, Italy
[37]INFN Sezione di Roma Tor Vergata, Roma, Italy
[38]Nikhef National Institute for Subatomic Physics, Amsterdam, Netherlands
[39]Nikhef National Institute for Subatomic Physics and VU University Amsterdam, Amsterdam, Netherlands
[40]AGH - University of Krakow, Faculty of Physics and Applied Computer Science, Kraków, Poland
[41]Henryk Niewodniczanski Institute of Nuclear Physics Polish Academy of Sciences, Kraków, Poland
[42]National Center for Nuclear Research (NCBJ), Warsaw, Poland
[43]Horia Hulubei National Institute of Physics and Nuclear Engineering, Bucharest-Magurele, Romania
[44]Authors affiliated with an institute formerly covered by a cooperation agreement with CERN
[45]ICCUB, Universitat de Barcelona, Barcelona, Spain
[46]La Salle, Universitat Ramon Llull, Barcelona, Spain
[47]Instituto Galego de Física de Altas Enerxías (IGFAE), Universidade de Santiago de Compostela, Santiago de Compostela, Spain
[48]Instituto de Fisica Corpuscular, Centro Mixto Universidad de Valencia - CSIC, Valencia, Spain
[49]European Organization for Nuclear Research (CERN), Geneva, Switzerland
[50]Institute of Physics, Ecole Polytechnique Fédérale de Lausanne (EPFL), Lausanne, Switzerland
[51]Physik-Institut, Universität Zürich, Zürich, Switzerland
[52]NSC Kharkiv Institute of Physics and Technology (NSC KIPT), Kharkiv, Ukraine
[53]Institute for Nuclear Research of the National Academy of Sciences (KINR), Kyiv, Ukraine
[54]School of Physics and Astronomy, University of Birmingham, Birmingham, United Kingdom
[55]H.H. Wills Physics Laboratory, University of Bristol, Bristol, United Kingdom
[56]Cavendish Laboratory, University of Cambridge, Cambridge, United Kingdom
[57]Department of Physics, University of Warwick, Coventry, United Kingdom
[58]STFC Rutherford Appleton Laboratory, Didcot, United Kingdom
[59]School of Physics and Astronomy, University of Edinburgh, Edinburgh, United Kingdom
[60]School of Physics and Astronomy, University of Glasgow, Glasgow, United Kingdom
[61]Oliver Lodge Laboratory, University of Liverpool, Liverpool, United Kingdom
[62]Imperial College London, London, United Kingdom
[63]Department of Physics and Astronomy, University of Manchester, Manchester, United Kingdom
[64]Department of Physics, University of Oxford, Oxford, United Kingdom
[65]Massachusetts Institute of Technology, Cambridge, Massachusetts, USA
[66]University of Cincinnati, Cincinnati, Ohio, USA
[67]University of Maryland, College Park, Maryland, USA
[68]Los Alamos National Laboratory (LANL), Los Alamos, New Mexico, USA
[69]Syracuse University, Syracuse, New York, USA
[70]Pontifícia Universidade Católica do Rio de Janeiro (PUC-Rio), Rio de Janeiro, Brazil (associated with Universidade Federal do Rio de Janeiro (UFRJ), Rio de Janeiro, Brazil)
[71]School of Physics and Electronics, Hunan University, Changsha City, China (associated with Institute of Particle Physics, Central China Normal University, Wuhan, Hubei, China)
[72]Guangdong Provincial Key Laboratory of Nuclear Science, Guangdong-Hong Kong Joint Laboratory of Quantum Matter, Institute of Quantum Matter, South China Normal University, Guangzhou, China (associated with Department of Engineering Physics, Tsinghua University, Beijing, China)
[73]Lanzhou University, Lanzhou, China (associated with Institute Of High Energy Physics (IHEP), Beijing, China)
[74]School of Physics and Technology, Wuhan University, Wuhan, China (associated with Department of Engineering Physics, Tsinghua University, Beijing, China)
[75]Henan Normal University, Xinxiang, China (associated with Institute of Particle Physics, Central China Normal University, Wuhan, Hubei, China)
[76]Departamento de Fisica, Universidad Nacional de Colombia, Bogota, Colombia (associated with LPNHE, Sorbonne Université, Paris Diderot Sorbonne Paris Cité, CNRS/IN2P3, Paris, France)
[77]Ruhr Universitaet Bochum, Fakultaet f. Physik und Astronomie, Bochum, Germany (associated with Fakultät Physik, Technische Universität Dortmund, Dortmund, Germany)
[78]Eotvos Lorand University, Budapest, Hungary (associated with European Organization for Nuclear Research (CERN), Geneva, Switzerland)
[79]Faculty of Physics, Vilnius University, Vilnius, Lithuania (associated with Physikalisches Institut, Albert-Ludwigs-Universität Freiburg, Freiburg, Germany)
[80]Van Swinderen Institute, University of Groningen, Groningen, Netherlands (associated with Nikhef National Institute for Subatomic Physics, Amsterdam, Netherlands)

[81]*Universiteit Maastricht, Maastricht, Netherlands*
(associated with Nikhef National Institute for Subatomic Physics, Amsterdam, Netherlands)
[82]*Tadeusz Kosciuszko Cracow University of Technology, Cracow, Poland*
(associated with Henryk Niewodniczanski Institute of Nuclear Physics Polish Academy of Sciences, Kraków, Poland)
[83]*Universidade da Coruña, A Coruña, Spain*
(associated with La Salle, Universitat Ramon Llull, Barcelona, Spain)
[84]*Department of Physics and Astronomy, Uppsala University, Uppsala, Sweden*
(associated with School of Physics and Astronomy, University of Glasgow, Glasgow, United Kingdom)
[85]*Taras Schevchenko University of Kyiv, Faculty of Physics, Kyiv, Ukraine*
(associated with Université Paris-Saclay, CNRS/IN2P3, IJCLab, Orsay, France)
[86]*University of Michigan, Ann Arbor, Michigan, USA*
(associated with Syracuse University, Syracuse, New York, USA)
[87]*Ohio State University, Columbus, USA*
(associated with Los Alamos National Laboratory (LANL), Los Alamos, New Mexico, USA)

[a]Deceased.
[b]Also at Lamarr Institute for Machine Learning and Artificial Intelligence, Dortmund, Germany.
[c]Also at Università degli Studi di Milano-Bicocca, Milano, Italy.
[d]Also at Università di Roma Tor Vergata, Roma, Italy.
[e]Also at Università di Modena e Reggio Emilia, Modena, Italy.
[f]Also at Università di Padova, Padova, Italy.
[g]Also at Università di Ferrara, Ferrara, Italy.
[h]Also at Universidade Estadual de Campinas (UNICAMP), Campinas, Brazil.
[i]Also at Università di Bologna, Bologna, Italy.
[j]Also at Università di Genova, Genova, Italy.
[k]Also at Università degli Studi di Milano, Milano, Italy.
[l]Also at Center for High Energy Physics, Tsinghua University, Beijing, China.
[m]Also at Universidad Nacional Autónoma de Honduras, Tegucigalpa, Honduras.
[n]Also at Università di Cagliari, Cagliari, Italy.
[o]Also at Centro Federal de Educacão Tecnológica Celso Suckow da Fonseca, Rio De Janeiro, Brazil.
[p]Also at Università di Bari, Bari, Italy.
[q]Also at Università di Perugia, Perugia, Italy.
[r]Also at LIP6, Sorbonne Université, Paris, France.
[s]Also at Università di Pisa, Pisa, Italy.
[t]Also at Hangzhou Institute for Advanced Study, UCAS, Hangzhou, China.
[u]Also at Scuola Normale Superiore, Pisa, Italy.
[v]Also at Università di Firenze, Firenze, Italy.
[w]Also at Università di Bergamo, Bergamo, Italy.
[x]Also at Universidad de Ingeniería y Tecnología (UTEC), Lima, Peru.
[y]Also at Università di Siena, Siena, Italy.
[z]Also at Università della Basilicata, Potenza, Italy.
[aa]Also at Universidad de Alcalá, Alcalá de Henares, Spain.
[bb]Also at Università di Urbino, Urbino, Italy.